In pancreatic islets from type 2 diabetes patients, the dampened circadian oscillators lead to reduced insulin and glucagon exocytosis

Volodymyr Petrenko[a,b,c,d], Nikhil R. Gandasi[e,f], Daniel Sage[g], Anders Tengholm[e], Sebastian Barg[e], and Charna Dibner[a,b,c,d,1]

[a]Division of Endocrinology, Diabetes, and Nutrition, Department of Medicine, University of Geneva, 1211 Geneva, Switzerland; [b]Department of Cell Physiology and Metabolism, Faculty of Medicine, University of Geneva, 1211 Geneva, Switzerland; [c]Diabetes Center, Faculty of Medicine, University of Geneva, 1211 Geneva, Switzerland; [d]Institute of Genetics and Genomics in Geneva, University of Geneva, 1211 Geneva, Switzerland; [e]Department of Medical Cell Biology, Uppsala University, 751 23 Uppsala, Sweden; [f]Department of Physiology, Institute of Neuroscience and Physiology, University of Göteborg, SE40530 Göteborg, Sweden; and [g]Biomedical Imaging Group, Ecole Polytechnique Fédérale de Lausanne, 1015 Lausanne, Switzerland

Edited by Joseph S. Takahashi, The University of Texas Southwestern Medical Center, Dallas, TX, and approved December 21, 2019 (received for review September 25, 2019)

Circadian clocks operative in pancreatic islets participate in the regulation of insulin secretion in humans and, if compromised, in the development of type 2 diabetes (T2D) in rodents. Here we demonstrate that human islet α- and β-cells that bear attenuated clocks exhibit strongly disrupted insulin and glucagon granule docking and exocytosis. To examine whether compromised clocks play a role in the pathogenesis of T2D in humans, we quantified parameters of molecular clocks operative in human T2D islets at population, single islet, and single islet cell levels. Strikingly, our experiments reveal that islets from T2D patients contain clocks with diminished circadian amplitudes and reduced in vitro synchronization capacity compared to their nondiabetic counterparts. Moreover, our data suggest that islet clocks orchestrate temporal profiles of insulin and glucagon secretion in a physiological context. This regulation was disrupted in T2D subjects, implying a role for the islet cell-autonomous clocks in T2D progression. Finally, Nobiletin, an agonist of the core-clock proteins RORα/γ, boosted both circadian amplitude of T2D islet clocks and insulin secretion by these islets. Our study emphasizes a link between the circadian clockwork and T2D and proposes that clock modulators hold promise as putative therapeutic agents for this frequent disorder.

circadian clock | exocytosis | human pancreatic islet | type 2 diabetes | real-time bioluminescence

The circadian clocks allow most of the organisms to anticipate periodical changes of geophysical time. In mammals, this time-keeping system governs most aspects of physiology and behavior. It comprises a master pacemaker, located in the paired suprachiasmatic nuclei (SCN) of the hypothalamus, that on a daily basis synchronizes peripheral oscillators situated in the organs (1). The circadian system orchestrates body metabolism via diverse neural and humoral pathways, thus ensuring the fine-tuning of the metabolic processes to the rest–activity and feeding–fasting cycles. In turn, the metabolites are feeding back on the circadian oscillators at the cellular and whole-body levels (2–6). Mouse strains lacking a functional clock due to the disruption of essential core-clock genes in the whole body, or in a tissue-specific manner, develop hyperglycemia, hypoinsulinemia, and glucose intolerance (7–10). Emerging works in humans suggest that a considerable portion of the transcripts in metabolic organs exhibit rhythmic expression (7, 11, 12). Human metabolomics and lipidomics studies have demonstrated diurnal profiles for a wide panel of metabolites in different peripheral tissues and in the blood (13–15). Moreover, epidemiological studies in humans strongly suggest that circadian misalignment may lead to the development of metabolic diseases, such as obesity and type 2 diabetes (T2D) (16, 17).

Several articles have provided a detailed characterization of molecular clocks operative in rodent pancreatic islets, highlighting primordial importance of functional islet clocks for insulin secretion and maintenance of glucose homeostasis (7, 8, 18). Such clock-mediated regulation of insulin secretion has been suggested to be exerted on insulin granule exocytosis, rather than on hormone synthesis, although direct evidence is still missing (7, 19, 20). Genetic mouse models with the pancreas-specific clock perturbation exhibit a phenotype of strongly disrupted insulin secretion, severe glucose intolerance, and all of the features of T2D from an early age, strongly suggesting implication of the islet clocks in T2D development (7, 8). Furthermore, the roles of the α-cellular clocks in regulating glucagon secretion in rodents have been highlighted, underscoring the importance of the interactions between the oscillators operative in α- and β-cells for islet function (20, 21). In line with these findings in rodents, studies in human islets unraveled the molecular makeup of the cell-autonomous local oscillators, and their primordial role in

Significance

Here we report that intact islets and islet cells from type 2 diabetes (T2D) donors exhibit attenuated molecular oscillators bearing lower circadian amplitude and compromised synchronization capacity in vitro. Furthermore, we reveal that secretion profiles of insulin, proinsulin, and glucagon were circadian rhythmic under physiological conditions. The temporal coordination of the islet hormone secretion was perturbed in human T2D islets, concomitant with the islet molecular clock alterations. Strikingly, clock-deficient human islet cells exhibited disrupted insulin and glucagon granule docking and exocytosis. Treating the T2D islets with the clock modulator Nobiletin boosted circadian amplitude and insulin secretion. Our study uncovers a link between human molecular clockwork and T2D, thus considering clock modulators as putative pharmacological intervention to combat this disorder.

Author contributions: V.P. and C.D. designed research; V.P. and N.R.G. performed research; A.T. contributed new reagents/analytic tools; V.P., N.R.G., D.S., S.B., and C.D. analyzed data; and V.P., S.B., and C.D. wrote the paper.

The authors declare no competing interest.

This article is a PNAS Direct Submission.

Data deposition: Raw data supporting the Fig. 5 and *SI Appendix*, Fig. S3 are deposited at http://dx.doi.org/10.17632/bwnrghvcpt.1.

[1]To whom correspondence may be addressed. Email: charna.dibner@hcuge.ch.

This article contains supporting information online at https://www.pnas.org/lookup/suppl/doi:10.1073/pnas.1916539117/-/DCSupplemental.

First published January 21, 2020.

functional regulation of the endocrine pancreas, notably in regulating insulin secretion (7, 12, 22). Experiments with human islets cultured in vitro revealed that upon clock disruption by RNA interference-mediated *CLOCK* knockdown human islet cells secreted less insulin. Furthermore, clock perturbation disrupted the rhythmicity of basal insulin secretion observed in islets of healthy human subjects (22). These data suggest a functional link between the pancreatic islet clock and insulin secretion and highlight the importance of islet oscillators in the development of T2D in rodents and possibly in humans.

In this study, we uncover the temporal coordination of insulin, proinsulin, and glucagon secretion profiles by the circadian oscillators operative in human islet cells. Such temporal coordination is likely exerted via an exocytosis process, since our experiments reveal that functional islet clocks are indispensable for proper secretory granule docking and exocytosis of insulin and glucagon. Strikingly, our study reveals that the circadian clockwork is compromised in human α- and β-cells in T2D, evidenced by the altered temporal profiles of insulin, proinsulin, and glucagon secreted by T2D human islets. Finally, the clock modulator Nobiletin shows a significant capacity to boost both the amplitude of circadian gene expression in human T2D islets and their insulin secretion, holding promise in terms of therapeutic implications.

Results

Circadian Oscillators Operative in Human Pancreatic Islet Cells Isolated from T2D Donors Exhibit a Dampened Amplitude and Altered Synchronization Properties.

We have previously identified molecular makeup of cell-autonomous circadian clocks operative in human islets at population, individual islet, and islet cell levels (12). In order to assess whether alterations may occur in the islet circadian clockwork concomitant with the development of T2D in humans, we first measured the expression levels of core-clock genes in nonsynchronized human islet cells derived from T2D donors, and compared those to nondiabetic (ND) counterparts (*SI Appendix*, Table S1). Expression levels of *PERIOD 1* to *3* (*PER1-3*), *CRY2*, *REV-ERBα*, *CLOCK*, and *DBP* were significantly diminished in T2D compared to ND islet cells (*SI Appendix*, Fig. S1*A*). *NFIL3* levels were slightly up-regulated, and *BMAL1* and *CRY1* did not change (*SI Appendix*, Fig. S1*A*).

Since expression levels of the key core-clock genes were strongly altered in T2D islets, we next assessed human islet clockwork by introducing two antiphasic circadian reporters, *Bmal1*-Luciferase (*Bmal1-luc*) or *Per2*-Luciferase (*Per2-luc*), allowing for continuous bioluminescence monitoring in human primary cells (23). In an agreement with previous clock characterization in human islets, primary skeletal myotubes, and skin fibroblasts (22, 24, 25), synchronization in vitro by forskolin pulse induced high-amplitude oscillations of both *Bmal1-luc* and *Per2-luc* reporters that were antiphasic in ND islets (compare ND lines in Fig. 1 *A* and *B*, *Left*). While both reporters were rhythmically oscillating in T2D islets following forskolin synchronization, the amplitude of these oscillations was significantly attenuated (Fig. 1 *A* and *B*). Absolute levels of *Bmal1-luc* expression were

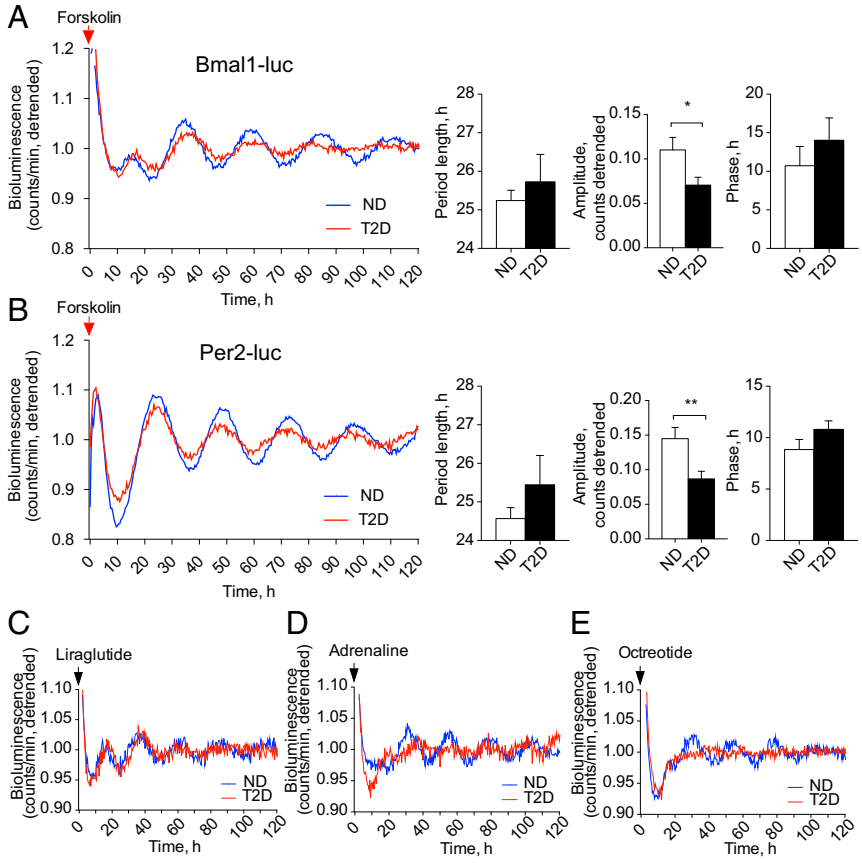

Fig. 1. Pancreatic islets derived from T2D human donors bear disrupted circadian clocks. (*A* and *B*) Average detrended oscillatory profiles of forskolin-synchronized human islet cells transduced with *Bmal1-luc* (*A*, $n = 19$ ND; $n = 15$ T2D donors) or with *Per2-luc* lentivectors (*B*, $n = 15$ ND; $n = 12$ T2D donors). Comparisons of average period length and amplitude are shown in adjacent histograms. $*P < 0.05$, $**P < 0.01$. (*C*–*E*) Average detrended *Bmal1-luc* bioluminescence profiles for pancreatic islets derived from ND and T2D donors synchronized in vitro with 1-h pulse of GLP-1 receptor agonist Liraglutide (*C*), adrenaline (*D*), or synthetic somatostatin analog Octreotide (*E*). See also *SI Appendix*, Fig. S1 and Table S2.

comparable and even slightly elevated in T2D islets (*SI Appendix*, Fig. S1*C*), whereas those of *Per2-luc* were strongly decreased in T2D islets compared to ND controls (*SI Appendix*, Fig. S1*D*). While no significant alterations in circadian period length and phase of *Per2-luc* oscillations have been observed overall between ND and T2D groups (Fig. 1 *B*, *Right*), nonsignificant tendencies of weak to moderate negative correlations between the circadian oscillation parameters and the blood levels of HbA1c measured in the same subjects have been observed within the T2D group (*SI Appendix*, Fig. S1 *F–H*).

Furthermore, we characterized *Bmal1-luc* reporter oscillatory profiles of ND control islets following synchronization by the pulses of Liraglutide, an analog of GLP-1, adrenaline, and Octreotide, an analog of somatostatin. Continuous recording of *Bmal1-luc* bioluminescence following Liraglutide, adrenaline, or Octreotide synchronization in ND islets (Fig. 1 *C–E* and *SI Appendix*, Table S2) revealed significant circadian oscillations as compared to the medium change alone (*SI Appendix*, Fig. S1*E*). Circadian amplitude of the oscillations induced by all three synchronizers was inferior to the one resulting from forskolin pulse (Fig. 1*A*). Period length was shorter for adrenaline-induced oscillations as compared to the other synchronizers, and phase was slightly advanced for adrenaline- and Octreotide-induced oscillations (compare Fig. 1 *A* and *D–E*; see also *SI Appendix*, Table S2). Importantly, when applied to T2D human islets, Octreotide failed to synchronize their clocks (Fig. 1*E*), whereas adrenaline pulse resulted in *Bmal1-luc* oscillations with a delayed circadian phase and tendency for dampened amplitude compared to ND controls (Fig. 1*D* and *SI Appendix*, Table S2). Reduced expression of *SSTR2* and *ADRA2A* receptor transcripts measured in T2D islets (*SI Appendix*, Fig. S1*B*) corroborated compromised synchronizing efficiency of adrenaline and somatostatin in T2D islets. Circadian oscillations resulting from Liraglutide pulse were comparable between ND and T2D islets (Fig. 1*C* and *SI Appendix*, Table S2), with significantly faster drop in amplitude by T2D islets as measured by the slope of peaks fading (-0.015 ± 0.0023 versus -0.007 ± 0.0018, $P = 0.024$).

Attenuated Individual Cell Oscillations and Perturbed Synchronization Capacity between the Endocrine Cellular Clocks Lead to the Impaired Islet Clockwork upon T2D. The perturbation of the islet oscillatory capacity observed in human T2D islets at the islet population level may stem from compromised islet cellular clockwork, or from disrupted synchronization capacity among the individual islets and individual islet cells upon T2D. To distinguish between these scenarios, we visualized *Per2-luc* oscillations of individual islets from T2D and ND donors synchronized by forskolin pulse employing bioluminescence time-lapse microscopy (Fig. 2 *A* and *B* and Movies S1 and S2). In line with our recordings at the islet population level (Fig. 1*B*), average profiles of *Per2-luc* oscillations in single T2D islets exhibited significantly lower circadian amplitude (Fig. 2 *C*, *Center*). Importantly, whereas oscillatory profiles of the individual ND islet clocks were in synchrony among the islets, the phase distribution of T2D islets was wider, indicating disrupted synchronization capacity among the T2D islets (Fig. 2 *C*, *Right*, and Movies S1 and S2). Overall, our single-islet recording experiments strongly suggest that T2D islets bear oscillators with lower circadian amplitude, and that synchronization among the individual T2D islet clocks by the most potent synchronizing agent forskolin is less efficient compared to ND counterparts.

In order to dissect the synchronization and individual oscillator properties in human α- and β-cells, Pppg-mCherry (26) and RIP-GFP (12) viruses were introduced, allowing for efficient and specific cell labeling. Combined bioluminescence-fluorescence time-lapse microscopy of human islet cells transduced with Pppg-mCherry, RIP-GFP, and *Per2-luc* viruses has been conducted (Fig. 2 *A* and *B* and Movies S1 and S2). *Per2-luc* profiles in the individual α- and β-cells from ND and T2D donors were traced using modification of a CGE algorithm (12, 27), and analyzed by JTK_Cycle (significance threshold of adjusted *P* value for JTK_Cycle analyses was set at 0.1). Most of the traced endocrine cells from ND (86 of 87 islet cells) and T2D donors (76 of 79 islet cells) were rhythmic. Importantly, circadian amplitude was strongly reduced in both α- and β-cellular clocks in the T2D group (Fig. 2 *D–F*), suggesting clockwork perturbation at the single-cell level. Moreover, both T2D α- and β-cells exhibited significant phase delay and wider phase distribution (Fig. 2*G*), indicative of less efficient synchronization capacity among the endocrine cells within T2D islets. Thus, both diminished circadian amplitude of individual islet cell clocks and wider phase distribution among the cells contribute to the compromised islet clockwork in T2D donors.

Human α- and β-Cells Synchronized In Vitro Secrete Glucagon, Insulin, and Proinsulin in a Circadian Rhythmic Manner. We recently revealed that human pancreatic islet cells synchronized in vitro exhibited a rhythmic profile of insulin secretion that was compromised in the absence of functional islet clocks (22). We now measured basal insulin secretion by isolated human β-cells. To this end, RIP-GFP–labeled human β-cells were separated by FACS, synchronized in vitro with forskolin pulse, and perifused during 48 h with a culture medium containing 5.5 mM of glucose (Fig. 3 *A* and *B*). Basal concentration of insulin secreted by human β-cells exhibited tendency for oscillations that did not reach statistical significance to qualify as circadian according to JTK_Cycle when applied to the time window 0 to 48 h (Fig. 3*B*). However, the oscillation pattern did qualify as circadian rhythmic in the time window between 4 and 48 h, evaluated to avoid a potential bias from immediate early response. Non-β (GFP^-)-cells from the same preparations secreted trace amounts of insulin, further validating the quality of β-cell population separation (Fig. 3*A*).

Next, we measured a temporal profile of glucagon secretion by a mixed human islet cell population (Fig. 3 *C* and *D*). Of note, glucagon was secreted in a significantly circadian rhythmic manner by human α-cells (Fig. 3 *C* and *D*). The insulin secretion profile by the same mixed islet cell population measured in parallel was rhythmic as well, with the phase of glucagon secretion peak being 2 h behind the peak of insulin secretion (Fig. 3 *C* and *D*).

In addition to mature insulin, β-cells secrete its nonprocessed precursor proinsulin. Our parallel measurements of proinsulin and insulin profiles by the same mixed islet cells revealed that also proinsulin secretion was circadian rhythmic (Fig. 3 *E* and *F*). The phase of proinsulin secretion profile was delayed about 2 h as compared to insulin in the same samples. Thus, our data provide evidence for circadian patterns of insulin, proinsulin, and glucagon secretion by human islet cells in physiological situation.

Circadian Profiles of Insulin, Proinsulin, and Glucagon Secretion Are Altered in T2D Islets. Next, temporal secretion profiles of insulin, glucagon, and proinsulin by T2D islet cells were assessed utilizing a perifusion system (Fig. 4 and *SI Appendix*, Fig. S2). Whereas a temporal pattern of insulin secretion by T2D islet cells still qualified as circadian by JTK_Cycle, the magnitude and overall amount of insulin secretion over 48 h were significantly diminished compared to ND controls. This difference was most prominent during the peak of insulin secretion (8 to 12 h and 32 to 36 h) (Fig. 4 *A* and *B* and *SI Appendix*, Fig. S2*D*). In line with compromised insulin secretion profiles, reduced expression of β-cell–specific genes *INS*, *MAFA*, and *SLC30A8*, and exocytosis-related genes *STX1*, *SNAP25*, and *VAMP2* was observed in nonsynchronized T2D islet cells (*SI Appendix*, Fig. S1*B*). While we did not detect a significant difference either in absolute values of glucagon secretion by T2D islet cells or in total glucagon

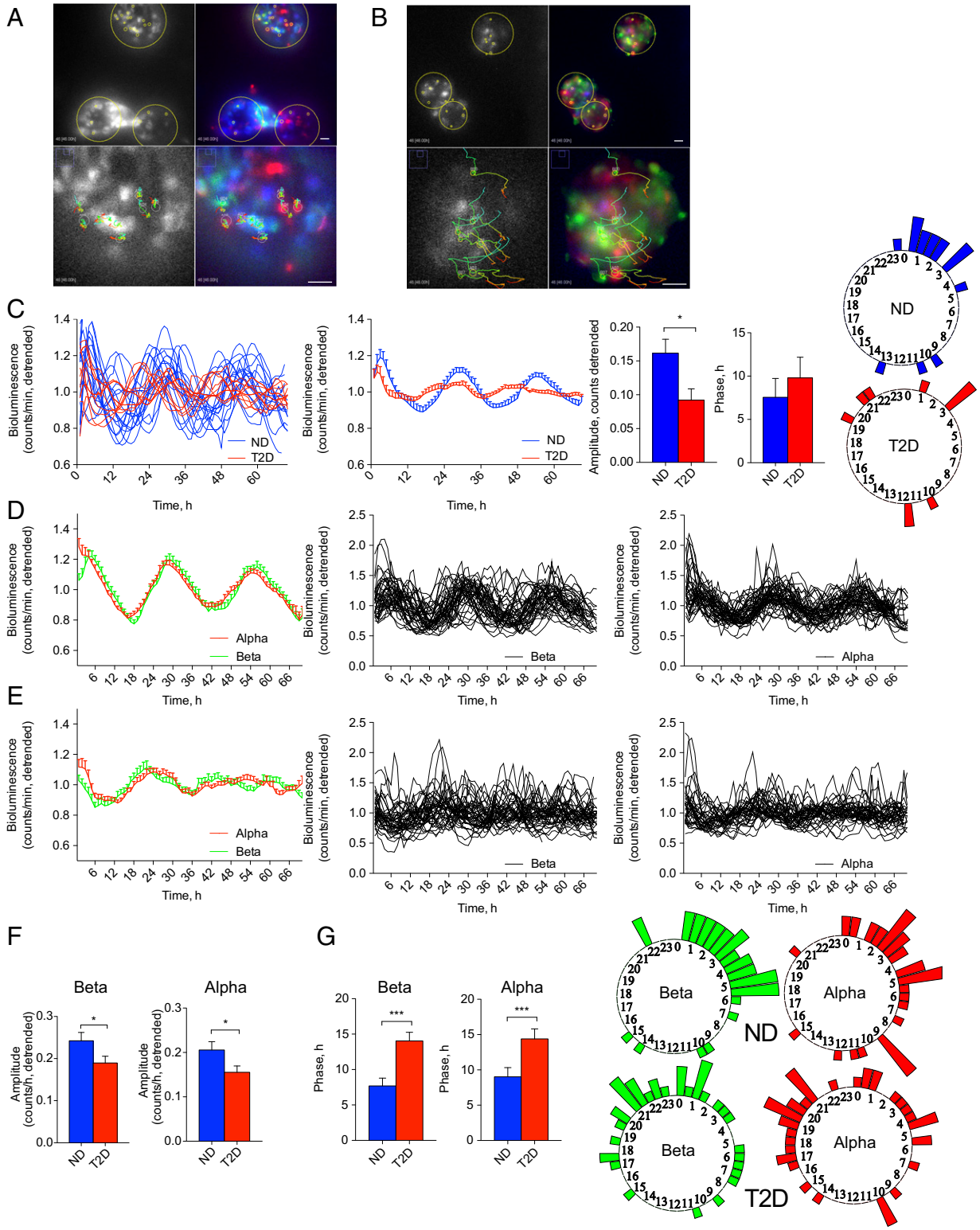

Fig. 2. The α- and β-cells constituting the islets from T2D human donors bear disrupted circadian oscillators. (*A* and *B*) Representative combined bioluminescence-fluorescence images of human islets from ND (*A*) and T2D (*B*) donors, subjected to time-lapse microscopy following forskolin synchronization (Movies S1 and S2). (Scale bars, 40 μm.) (*C*) Average *Per2-luc* bioluminescence expression profiles of single human islets in $n = 6$ ND and $n = 5$ T2D donors (Movies S1 and S2). (C, *Left*) Individual islet profiles ($n = 17$ for ND donors, $n = 11$ for T2D donors); (*Center*) the average profiles for islets from all ND and T2D donors and histograms comparing their average amplitudes and phases. Phase distribution of individual islets from ND and T2D donors is presented on the adjacent polar histograms (*Right*). (*D* and *E*) Average (*Left*) and individual *Per2-luc* bioluminescence profiles for β-cells (*Center*) and α-cells (*Right*) from ND (*D*) and T2D donor islets (*E*). Average circadian amplitude (*F*), and phase (*G*) for all analyzed single α-cells and β-cells from ND and T2D donors. Phase distribution of individual islet cells (α- and β-) from ND and T2D donors is presented on the polar histograms adjacent to *G*. $^{*}P < 0.05$, $^{***}P < 0.001$.

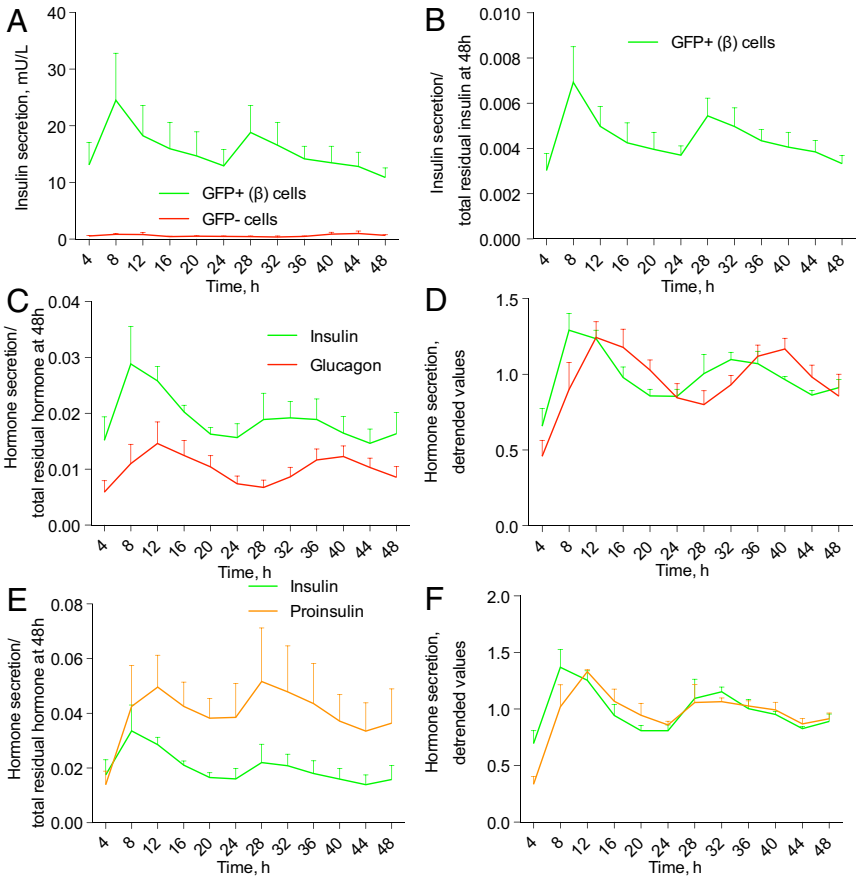

Fig. 3. Glucagon, insulin, and proinsulin are rhythmically secreted by human islet cells synchronized in vitro. (*A*) Temporal insulin secretion profile by FACS-separated human β-cells (~25,000 cells per dish) assessed by perifusion. (*B*) Insulin secretion values presented in *A* were normalized to the total hormone content in the cell lysate at the end of the experiment (at 48 h). When JTK_Cycle was applied to the time window 4 to 44 h, to exclude a possible bias due to immediate-early response to synchronization, the resulting profile of insulin secretion qualified as circadian rhythmic ($P = 0.084$), with the average period length 24.04 ± 0.98 h, and phase 10.4 ± 4.62 h. (*C*) Insulin and glucagon secretion by ~50,000 mixed ND islet cells from $n = 6$ donors subjected to perifusion and normalized to residual respective hormone content at 48 h (*C*). Note the delayed phase of glucagon secretion as compared to insulin ($P = 0.0019$, paired Student's *t* test). (*E*) Insulin and proinsulin secretion by ND islet cells from $n = 4$ donors. Note the delayed phase of proinsulin secretion as compared to insulin ($P = 0.02$, paired Student's *t* test). (*D* and *F*) Detrended values from *C* and *E*. JTK_Cycle qualified as circadian rhythmic the average profile of insulin (*D*, $P = 0.057$; period length 22.96 ± 0.75 h); of glucagon (*D*, $P = 0.009$, period length 24.3 ± 0.22 h); and of proinsulin (*F*, $P = 0.097$, period length 21.5 ± 0.96 h).

content in T2D islet cells, the temporal profile of glucagon secretion was altered (Fig. 4 *C* and *D* and *SI Appendix*, Fig. S2 *C* and *E*). Indeed, the circadian rhythmicity of glucagon secretion by T2D islet cells was lost (Fig. 4*D*). Finally, the proinsulin secretion profile by T2D islet cells was not qualified as circadian rhythmic according to the JTK_Cycle (Fig. 4 *E* and *F* and *SI Appendix*, Fig. S2*F*).

Functional Clock Is Required for Insulin and Glucagon Granule Docking and Exocytosis in Pancreatic α- and β-Cells. Down-regulation of the *CLOCK* gene has been recently shown to affect expression of genes coding for components of the insulin granule exocytosis machinery (22). We therefore quantified granule docking and exocytosis by total internal reflection fluorescence (TIRF) microscopy in ND human β-cells, in which *CLOCK* was knocked down using small-interfering RNA (siRNA). The granules were labeled by transducing the cells with the adenoviral granule marker NPY-mCherry (28), and α- or β-cells were identified by using cell specific promoters driving the expression of fluorescent proteins (*Materials and Methods*). β-Cells showed a pronounced decrease in the density of plasma membrane-docked granules under *CLOCK* knockdown (by 34%, $P < 0.0005$) (Fig. 5 *A* and *B*). The trend was similar in α-cells that also showed a slight decrease in the density of plasma membrane-docked granules in *CLOCK* knockdown condition ($P < 0.05$) (Fig. 5 *F* and *G*).

We then stimulated exocytosis by elevating extracellular K^+ to 75 mM for 40 s. Single exocytosis events were observed as a sudden disappearance of granule fluorescence (example in Fig. 5 *C* and *E*) (29, 30). As reported previously (28), in control β-cells the rate of exocytosis was initially high but slowed toward the end of the stimulation (Fig. 5*D*). On average, 0.13 (±0.016) exocytosis events were recorded during the stimulation in control cells (Fig. 5*E*). In *siCLOCK*-transfected cells, both the rapid and the slow phases were still present, but exocytosis was strongly reduced (85% to 0.02 ± 0.004 g/μm^2, $P < 0.0005$). In α-cells, we observed a similarly strong reduction in K^+-stimulated exocytosis after knockdown of *CLOCK* (82% to 0.014 ± 0.003 g/μm^2, $P < 0.0005$) (Fig. 5 *H* and *I*).

Exocytosis and granule docking were also quantified in islets from mice in which *Bmal1* was deleted (Bmal1KO). In β-cells, docked granules were reduced by 34% (*SI Appendix*, Fig. S3 *A* and *B*), and K^+-stimulated exocytosis was reduced by 46% (*SI Appendix*, Fig. S3*C*). In α-cells of Bmal1KO mice we observed a similar tendency with reduction of both docked granules (by 20%) (*SI Appendix*, Fig. S3 *D* and *E*) and K^+-stimulated exocytosis (by 82%) (*SI Appendix*, Fig. S3*F*). Collectively, these results further indicate that CLOCK and BMAL1, the two members

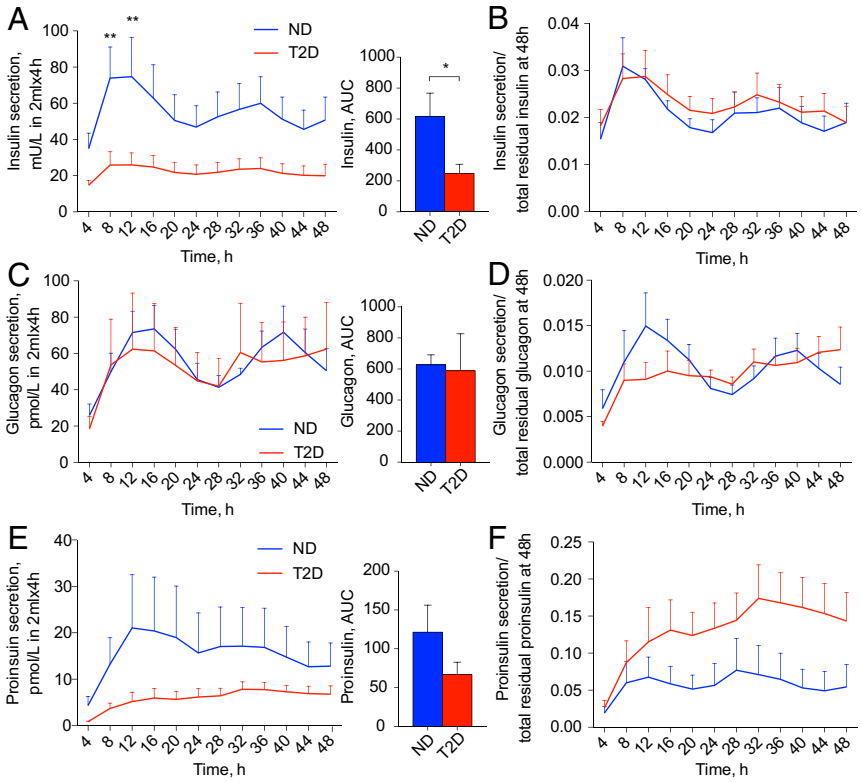

Fig. 4. Circadian rhythmic profiles of insulin, proinsulin, and glucagon secretion are disrupted in T2D. Secretion profiles of insulin (*A* and *B*, $n = 6$ ND; $n = 10$ T2D donors), glucagon (*C* and *D*, $n = 6$ ND; T2D donors), and proinsulin (*E* and *F*, $n = 4$ ND; $n = 5$ T2D donors) were measured in the outflow perifusion medium from ~50,000 synchronized mixed human islet cells. (*B*, *D*, and *F*) Respective raw data from *A*, *C*, and *E* were normalized to the total hormone content in the cell lysate at the end of each experiment. JTK_Cycle analysis qualified insulin secretion profile in ND islets as circadian rhythmic ($P = 0.097$), with the amplitude of 0.006 ± 0.0015 relative units, period length 23.68 ± 0.96 h, and phase 8.41 ± 1.05 h. Whereas the insulin secretion profile was still qualified as circadian rhythmic in T2D donors ($P = 0.097$), the amplitude of these oscillations was strongly diminished to 0.0038 ± 0.0012 relative units; period length of 23.67 ± 0.63 h and phase 9.76 ± 0.8 h. Glucagon secretion profile qualified as circadian rhythmic in ND donors ($P = 0.009$), with amplitude 0.0045 ± 0.0014, period length 24.3 ± 0.22 h, and phase 10.94 ± 1.23 h, whereas it was nonrhythmic in T2D donors ($P = 0.81$). Proinsulin secretion profile in ND donors was qualified as circadian ($P = 0.097$) with amplitude of 0.014 ± 0.0048; period length 21.5 ± 0.96 h, and phase 10.5 ± 1.5 h, while in T2D donors it was considered noncircadian ($P = 1$). See also *SI Appendix*, Fig. S2. $*P < 0.05$, $**P < 0.01$.

of the positive limb of the molecular oscillator, are required for proper functioning of the insulin and glucagon granule exocytosis machinery.

High Glucose Levels Alter Molecular Clocks in the Islets from ND, but Not from T2D Donors. To assess the effect of high glucose on the islet clockwork, we recorded *Bmal1-luc* or *Per2-luc* oscillations from ND islets in the presence of 20 mM glucose. Adding high glucose to recording medium resulted in 1 h longer circadian period length for both reporter profiles compared to the physiological concentration of 5.5 mM (Fig. 6*A* and *SI Appendix*, Fig. S4*A*). In contrast, the oscillatory profiles of T2D islets in the presence of 5.5 mM (low) and 20 mM (high) glucose in the recording medium were comparable, suggesting that high glucose levels do not induce significant changes in the clockwork (Fig. 6*B* and *SI Appendix*, Fig. S4*B*).

When perifused with high glucose, ND islet cells secreted significantly higher insulin levels comparatively to their counterparts perifused with low glucose. This difference was particularly striking during the insulin secretion peaks between 8 to 12 h and 28 to 32 h (Fig. 6*C*). Interestingly, insulin secretion reached its maximum 2 to 4 h prior to the peak of *Per2-luc* expression recorded in parallel from the same cells (*SI Appendix*, Fig. S4*C*). In contrast, T2D islet cells perifused with high glucose secreted only slightly more insulin than their counterparts perifused with low glucose (Fig. 6*C* and *SI Appendix*, Fig. S4*D*). In an agreement with the outcome of perifusion experiments, static insulin secretion by nonsynchronized T2D islet cells was slightly elevated in the presence of low glucose, whereas it was decreased at high glucose. This led to a 2.5-fold lower stimulation index for T2D islets (Fig. 6*D* and *SI Appendix*, Fig. S4*F*). Impaired glucose sensitivity of the T2D islet cells might be partly attributed to altered expression levels of insulin-independent glucose transporters *GLUT1* and *GLUT2* in T2D islet cells (*SI Appendix*, Fig. S1*B*) observed in our samples, consistently with the previous reports (31). No significant difference in the islet cell apoptosis has been observed following incubation with high glucose (*SI Appendix*, Fig. S4*E*). Collectively, these data indicate that high glucose interferes with the pancreatic islet cell clockwork in ND by lengthening the period, but has little effects on either oscillation of clock gene expression or on temporal insulin secretion in T2D islets.

In Human T2D Islets the Receptor-Related Orphan Receptor Agonist Nobiletin Boosts the Amplitude of Circadian Gene Expression and Increases Basal and Stimulated Insulin Secretion. To examine whether boosting the T2D islet clockwork may have a beneficial effect on insulin secretion, we attempted to restore the dampened circadian amplitude in T2D islets pharmacologically. To this end, we employed Nobiletin, a drug that has been shown to enhance circadian amplitude in clock-deficient mouse fibroblasts via receptor-related orphan receptor (ROR) nuclear receptors (32). Assessment of the expression levels of *RORα* transcripts revealed no change between ND and T2D islets (*SI Appendix*,

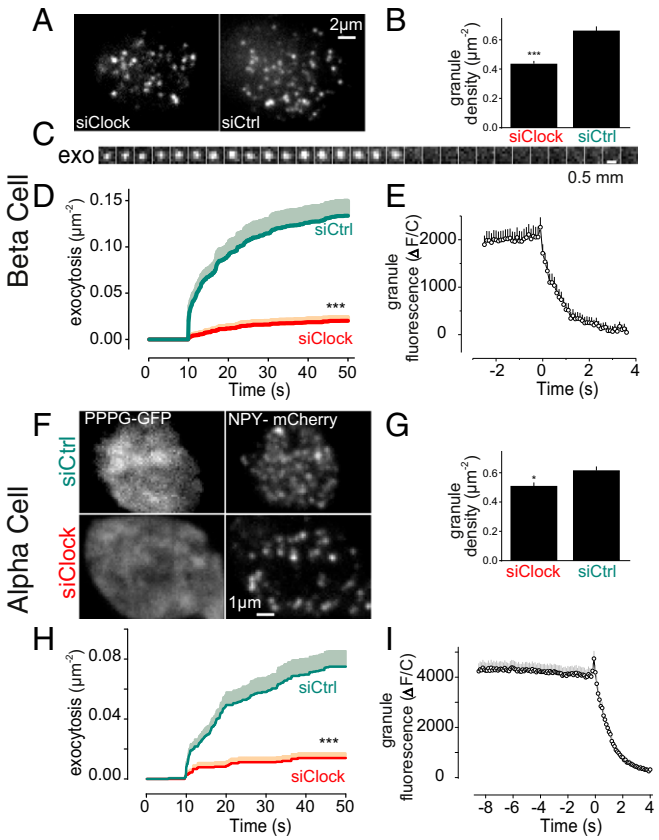

Fig. 5. Molecular clock affects granule docking and exocytosis in human α- and β-cells. (*A*) β-Cells from nondiabetic donors transfected with siRNA targeting *CLOCK* gene (siClock), or scrambled control siRNA (siCtrl). (*B*) Density of docked granules in cells as in *A*. (*C*) Image sequence (0.1 s per frame) showing an individual insulin granule undergoing K^+-stimulated exocytosis (exo). (*D*) Time course of exocytosis constructed from events as in *C*, in response to elevation of K^+ to 75 mM for 40 s, 10 s after the experiment was initiated. (*E*) Average granule fluorescence from all of the exocytosis events seen in siCtrl in *D*. Note the disappearance of fluorescence signal at time 0. (*F*) α-Cells of ND donors identified by expression of Pppg-GFP (*Left*) and coexpressing the granule marker NPY-mCherry (*Right*) and either transfected with scrambled control (siCtrl, *Upper*), or siRNA targeting *CLOCK* (siClock, *Lower*). (*G*) Density of docked granules. (*H*) Time course of exocytosis in α-cells as in *F*. (*I*) Average granule fluorescence from all of the exocytosis events seen in siCtrl in (*H*). Note the disappearance of fluorescence signal at time 0. $*P < 0.05$, $***P < 0.001$. See also *SI Appendix*, Fig. S3.

Fig. S1*A*). When applied to synchronized T2D human islets, Nobiletin doubled the magnitude and significantly enhanced the amplitude of *Bmal1-luc* oscillations at least during the first two cycles (Fig. 7 *A* and *B*). Similar trend for magnitude was observed for the islets from both ND and T2D donors transduced with *Per2-luc* reporter; however, the effect on circadian amplitude did not reach statistical significance in this case (*SI Appendix*, Fig. S5 *A* and *B*). Noteworthy, Nobiletin acutely boosted *Bmal1-luc* expression when applied to forskolin-synchronized T2D islets (*SI Appendix*, Fig. S5*C*). Long-term application of Nobiletin to ND and T2D islets did not result in any detectable increase in the islet cell apoptosis (*SI Appendix*, Fig. S5*D*).

Next, we investigated the effect of Nobiletin on insulin secretion by human islets. Adding Nobiletin to the medium containing 5.5 mM glucose led to 3.5-fold increase in insulin secretion by ND islets (Fig. 7*C*). In concordance with static insulin release, a glucose-stimulated insulin secretion (GSIS) test showed significant rise in insulin secretion in basal (fivefold) and glucose-stimulated (twofold) conditions (Fig. 7*D*). Increased insulin secretion did not stem from the effect on insulin production de novo since the total amount of produced insulin during both tests in the presence of Nobiletin was comparable to the control condition (*SI Appendix*, Fig. S5 *E* and *F*). Subsequently, we tested the capacity of Nobiletin to boost insulin secretion in *siCLOCK* expressing islet cells that exhibited reduced basal and stimulated insulin secretion (22). GSIS tests conducted in *siCLOCK*-transfected ND islet cells in the presence of Nobiletin resulted in a marked enhancement of basal and stimulated insulin secretion (Fig. 7*E*). Remarkably, Nobiletin ameliorated the compromised capacity by T2D islets to release insulin at basal glucose conditions and in the GSIS test (Fig. 7 *F* and *G* and *SI Appendix*, Fig. S5 *E* and *F*). Overall, Nobiletin partly restored compromised basal and GSIS by human T2D islets and ND islets bearing disrupted clocks and further enhanced insulin secretion by human ND islets. Noteworthy, Nobiletin also induced glucagon secretion in ND and T2D islets during glucagon release test in the presence of 5.5 mM glucose (*SI Appendix*, Fig. S5*G*). Furthermore, we utilized SR9011, a synthetic agonist of *REV-ERB* receptors (33). Contrary to Nobiletin, SR9011 diminished the magnitude of *Per2-luc* reporter expression by ND islets, without notable dampening of the circadian amplitude (*SI Appendix*, Fig. S5*H*). Of note, application of SR9011 to T2D islet cells throughout all of the stages of GSIS assay significantly reduced the insulin secretion capacity of these cells (Fig. 7*H*).

Discussion

Rodent studies reported a critical role of the islet circadian clocks in maintaining glucose homeostasis, concomitant with the link between disruption of the islet oscillators and the development of T2D (1, 5, 34). Here we provide a convincing evidence that pancreatic islets isolated from human T2D donors exhibit strongly diminished amplitude of circadian oscillations, as compared to ND counterparts. Furthermore, synchronization capacity of T2D islets by physiologically relevant compounds was reduced. Along with the observed disruption of circadian oscillators, temporal profiles of insulin, proinsulin, and glucagon secretion, that are rhythmic in the case of ND islets, were perturbed in T2D islets. Pancreatic islet oscillators are likely regulating the hormone secretion via the exocytosis process. Indeed, in the model of the islet clock disruption, insulin and glucagon granule docking and exocytosis were strongly decreased, similar to the phenotype observed in T2D islets. Strikingly, the clock modulator Nobiletin enhanced the amplitude of *Bmal1-luc* circadian oscillations in T2D islets, and partly restored insulin secretory capacity of these islets.

Cell-Autonomous Clocks in Pancreatic Islets Isolated from T2D Donors Exhibit Diminished Circadian Amplitude and Reduced Synchronization Capacity. Pancreatic islets receive numerous systemic and paracrine physiological signals that couple the function of the endocrine pancreas to the metabolic needs on a daily basis, possibly via modulating circadian rhythmicity of α- and β-cells. Indeed, physiologically relevant stimuli such as adrenaline, insulin, glucagon, somatostatin, and GLP-1 analogs (Liraglutide and Exenatide) differentially reset mouse α- and β-cell molecular clocks (20, 21). Forskolin, dexamethasone, and temperature cycles have been shown to efficiently synchronize human pancreatic islet clocks in vitro (7, 12). Here we demonstrate that adrenaline, Octreotide, and Liraglutide are potent synchronizers of circadian clocks in ND human islets. Our data also indicate that chronic application of high glucose levels on ND islets lengthens the circadian period of human islet clocks. The effect of glucose on the islet clocks might be mediated via down-regulation of *Per1* and *Per2* transcripts, as was reported for cultured fibroblasts (35). In mice, islet cellular clocks in FACS-separated α- and β-cell populations exhibit distinct circadian properties and

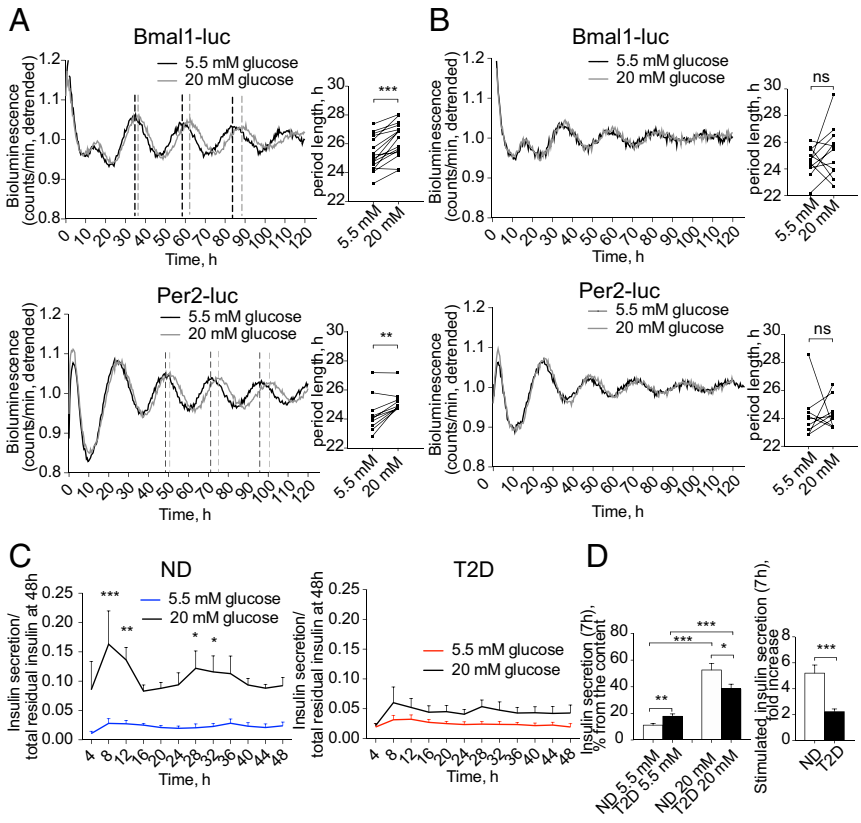

Fig. 6. High glucose levels impact on the molecular clocks in the islets from ND, but not from T2D donors. Average detrended oscillatory profiles of forskolin-synchronized human islet cells from ND (*A*) and T2D donors (*B*) transduced with *Bmal1-luc* (*Upper*, $n = 15$ for ND and $n = 10$ for T2D) or *Per2-luc* lentivectors (*Lower*, $n = 9$ for ND and $n = 8$ for T2D). Adjacent histograms show changes in the period length of islet oscillations recorded in the presence of 20 mM glucose in the medium (difference is tested by paired Student's *t* test). (*C*) Insulin secretion by mixed islet cells synchronized with forskolin and perifused in parallel with the medium containing either 5.5 mM or 20 mM glucose across 48 h ($n = 3$ of ND and $n = 5$ T2D donors). Two-way ANOVA test with Bonferroni posttest was used to assess the difference between experimental conditions. (*D*) Static release (*Left*) of insulin by dispersed islet cells from ND or T2D donors was measured after 7-h incubation in the presence of 5.5 or 20 mM glucose, and expressed as percent of total residual insulin content in the end of the experiment (mean ± SEM) for $n = 10$ ND and $n = 10$ T2D preparations. Respective stimulation index is expressed (*Right*). $^*P < 0.05$, $^{**}P < 0.01$, and $^{***}P < 0.001$. ns, not significant. See also *SI Appendix*, Fig. S4.

differential responses to physiologically relevant synchronizers (20, 21). Utilizing time-lapse microscopy, we now report that within intact human islets, α- and β-cells possess oscillators with comparable circadian properties, implying the role of the islet cytoarchitecture and paracrine interactions among different endocrine cells for the circadian coupling, similar to those observed in SCN neurons. Although the exact mechanism of coupling among cellular clocks in SCN is not entirely understood, it involves Na^+-dependent action potentials relying on the activity of voltage-dependent calcium channels in response to chemical stimuli and transmission of the electrical signaling via gap-junctions (36). Similarly, the coordinated secretory response by the islet to glucose stimulation requires intraislet cell coupling via gap-junctions (37). Furthermore, paracrine glucagon and GLP-1 signaling emanating from α-cells is indispensable for efficient regulation of glucose homeostasis by neighboring β-cells (38). Given that glucose, insulin, adrenaline, glucagon, somatostatin, and GLP-1 mimetics efficiently reset pancreatic islet clocks in mouse and human islets (20, 21), the signaling pathways induced by these molecules might be good candidates for mediators of both circadian and functional coupling among the islet cells.

Pancreatic islets derived from T2D donors exhibited attenuated circadian rhythms as compared to ND counterparts (Figs. 1 and 2 and *SI Appendix*, Fig. S1). In line with previous transcriptomic screening (39), we also show that expression of core-clock components is strongly altered in nonsynchronized cultured human T2D islets (*SI Appendix*, Fig. S1*A*). Observed suppression of one or several components in the principal core-clock loop (*CLOCK*, *PER1-2*) may account for dampening the circadian reporter amplitude observed in synchronized T2D islets, as has been previously demonstrated in the skin fibroblasts derived from respective mouse KO models (40, 41). Beyond observed perturbation in the clockwork per se, T2D islet clock oscillators failed responding to physiologically relevant molecules, such as adrenalin, Octreotide, and glucose, further compromising their ability to anticipate and adequately react to feeding–fasting cycles. Loss of the adrenergic resetting effect on the T2D islet clocks might be associated with reduction of *ADRA2A* expression (*SI Appendix*, Fig. S1*B*) (42), or with genetic variant of *ADRA2A* found in a subset of T2D patients characterized by enhanced adenylate cyclase inhibitory activity in β-cells (43). Similarly, alteration of somatostatin resetting effect on islet clocks might be attributed to reduction of *SSTR2* expression levels in T2D islet cells (*SI Appendix*, Fig. S1*B*) (42). Furthermore, changes of *GLUT2* and *GLUT1* transporter expression in T2D islets (*SI Appendix*, Fig. S1*B*) (44) may account for the lack of response by the islet cellular oscillators to the high glucose in the medium that was observed in T2D islets, contrary to the ND counterparts (Fig. 6). Of note, while glucose, adrenaline, and somatostatin fail to efficiently synchronize human T2D islet clocks, the GLP-1R mimetic Liraglutide maintained its resetting capacity on T2D oscillators, extending its therapeutic action to the

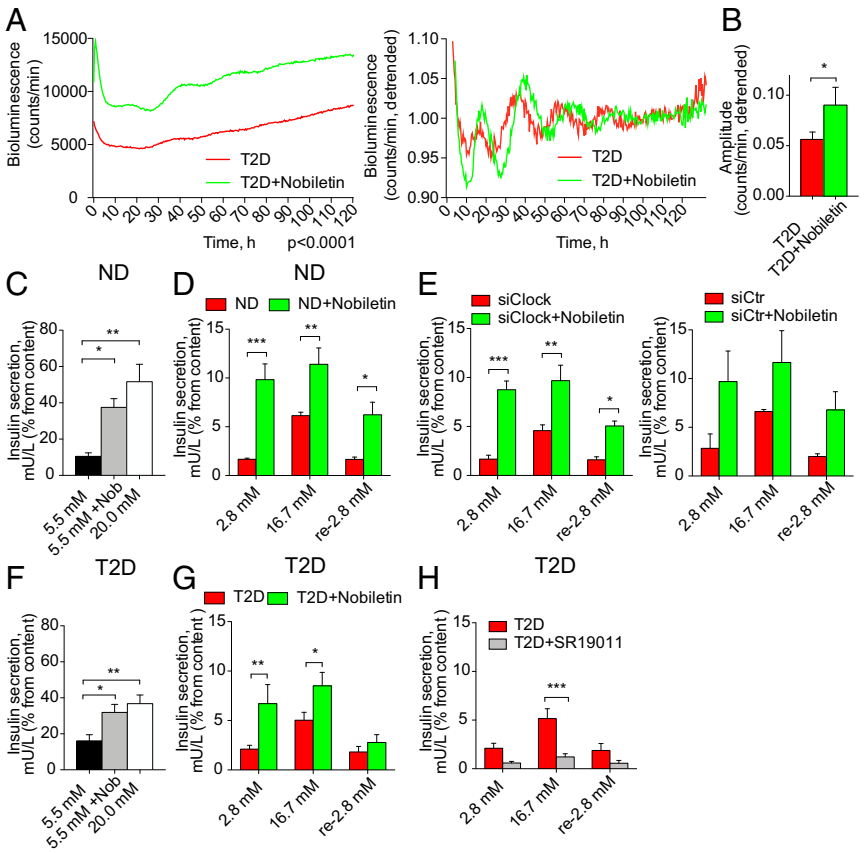

Fig. 7. The ROR agonist Nobiletin boosts disrupted molecular oscillators in human T2D islets, and enhances basal and stimulated insulin secretion by these islets. (*A*) Nobiletin enhances magnitude (*Left*) and amplitude (*Right*) of *Bmal1-luc* reporter oscillations in T2D islets synchronized with forskolin ($n = 4$ islet batches from individual T2D donors). Difference in circadian magnitude (*Left*) was tested using two-way ANOVA test, $P < 0.0001$. Difference in circadian amplitude is shown in the adjacent histogram (*B*). (*C* and *D*) Stimulatory effect of Nobiletin on long-term (*C*, 7 h) and short-term (*D*, 1 h) insulin secretion by human islet cells from ND donors ($n = 4$). (*E*) Effect of Nobiletin on glucose-induced insulin secretion in human islet cells transfected with siRNA targeting *CLOCK* leading to the clock perturbation (22, 23). Insulin secretion by *siCLOCK*-transfected human islet cells (*Left*, $n = 3$ independent experiments), or by counterparts treated with scrambled siRNA (siCtr, *Right*, $n = 2$ independent experiments). Data are expressed as mean ± SEM (*F* and *G*) Nobiletin stimulates insulin release by T2D islet cells during static 7 h incubation (*F*, $n = 5$ donors), and in short-term glucose-induced insulin secretion tests (*G*, $n = 5$ donors). See also *SI Appendix*, Fig. S5. (*H*) REV-ERBs agonist SR9011 dampens glucose-induced insulin secretion by T2D human islet cells during 1 h. Data are expressed as mean ± SEM, $n = 4$ donors. The difference is tested by two-way ANOVA test with Bonferroni posttest. *$P < 0.05$, **$P < 0.01$, and ***$P < 0.001$.

islet clock modulating function. Interestingly, the oscillation period length within the T2D group showed a tendency for inverse correlation with the T2D severity measured by blood HbA1c levels in the same donors (*SI Appendix*, Fig. S1*G*) that did not reach statistical significance. A similar negative correlation was observed between period length of cultured skin fibroblasts and blood HbA1c in a different cohort of T2D donors (24).

Perturbed Circadian Oscillators in Human T2D Islets May Affect Temporal Hormone Secretion via Regulating the Islet Hormone Exocytosis. Blood levels of insulin exhibit pronounced daily rhythmic profiles in rodents and in healthy human volunteers (8, 20, 45). These oscillatory profiles are stemming, at least in part, from rhythmic insulin secretion, as was shown by in vitro experiments with isolated mouse and human islets. The latter are compromised in the absence of functional islet clocks (8, 22), suggesting a primordial role of the cell-autonomous circadian oscillators for islet function. Here we show that concordantly with rhythmic secretion of insulin by mixed human islet cells and by pure mouse β-cells, also pure human β-cells synchronized in vitro secrete insulin in a circadian fashion. Additionally, circadian profile of proinsulin secretion was ∼2-h phase-delayed compared to insulin secreted by the same islets. Oral glucose tolerance test in humans revealed that release of unprocessed proinsulin follows the one of mature insulin (46), likely reflecting an additional recruitment of proinsulin-containing immature granules upon increased insulin needs. Finally, we show that human islet cells secret glucagon in a circadian fashion. The peak of the rhythmic secretory profile of glucagon was delayed in comparison to that of insulin secreted by the same islets, in agreement with the data in rodents (20, 47). Importantly, rhythmic temporal profiles of proinsulin, insulin, and glucagon secretion by synchronized ND islets were strongly compromised in the T2D islets. In agreement with the data in first-degree relatives of T2D patients, pointing to the absence of the ascending phase of circadian rhythm and the attenuation of the circadian amplitude of insulin secretion rate (48), we found decreased magnitude and amplitude of insulin secretion in T2D islets synchronized in vitro. Strikingly, the circadian rhythmic profile of basal insulin secretion by ND islets was compromised following induced attenuation of molecular clocks (22), providing a parallel between the islet hormone secretion phenotype associated with T2D and with siRNA-mediated islet clock disruption.

Furthermore, our experiments suggest that functional islet clocks are indispensable for a proper docking and exocytosis of insulin and glucagon granules in humans and in mice. Indeed, *siCLOCK*-mediated clock disruption in human islets and *Bmal1* knockout in mice resulted in a similar phenotype comprising

strong decrease in the secretory granule docking and of exocytosis events (Fig. 5 and *SI Appendix*, Fig. S3). The docking defect in β-cells was more pronounced than in α-cells. In line with these findings, transcriptomic analyses revealed that a large portion of key regulators of the secretory granule trafficking, docking, and exocytosis is under clock regulation in mouse and human islets (6, 7, 20, 22). In concordance with our data (*SI Appendix*, Fig. S1*B*), the impaired expression of similar groups of genes involved in exocytosis was shown in T2D islets (49) and upon islet clock disruption (22). Thus, the phenotype observed by us in ND human islets bearing disrupted clocks (Fig. 5) recapitulates changes described in human islet cells derived from T2D donors, where reduced granule docking limited sustained insulin secretion (28). The intriguing parallel between the islet transcriptional and functional alterations in human T2D and in human islets bearing compromised clocks supports a potential role of the cell-autonomous islet oscillators in the islet function, glucose homeostasis, and pathogenesis of T2D.

Human studies in controlled laboratory conditions highlighted that even short-term circadian misalignment leads to glucose intolerance and development of metabolic diseases (50). Moreover, disruption of the human islet molecular clocks in vitro attenuates basal and stimulated insulin secretion (22). This work provides evidence linking circadian clock disruption to compromised temporal and absolute levels of islet hormone secretion in the pathogenesis of T2D in humans.

Restoring T2D Islet Oscillators and Insulin Secretion with the Clock Modulator Nobiletin. The ROR nuclear receptor agonist Nobiletin exhibited multiple beneficial effects in rodent models, protecting against development of atherosclerosis, obesity, metabolic syndrome, and insulin resistance in rodents (32, 51, 52). Here we show that the clock modulator Nobiletin efficiently restores flattened amplitude of circadian oscillations in human T2D islets. Strikingly, Nobiletin also enhanced basal and glucose-stimulated insulin secretion in the same T2D islets, and in the islets obtained from ND donors following si*CLOCK*-mediated clock disruption. In line with original report on metabolic effects of Nobiletin on db/db Clock mutant mice (32), these data suggest that effects of Nobiletin on insulin secretion might be at least partly attributed to the core-clock unrelated action of ROR nuclear receptors. This hypothesis is further supported by the observation that REV-ERB agonist SR9011 exerted inhibitory effect on insulin secretion as opposed to Nobiletin, which was not paralleled by any significant changes in *Per2-luc* oscillation amplitude. Additionally, recently published RNA-sequencing analyses revealed up-regulation of ROR target genes in skeletal muscle following Nobiletin treatment, comprising the genes encoding for the core-clock components, mitochondrial electron transport chain, and reactive oxygen species scavenging (53). Activation of mitochondrial electron transport chain may potentially represent the clock-unrelated mechanism of Nobiletin action in the islet cells upon clock perturbation. Our in vitro data in human islets, and in vivo treatment of rodents with Nobiletin showed no notable toxicity for this compound (32). Of note, continuous stimulation of insulin secretion exerted by Nobiletin may exhaust the dysfunctional β-cells in T2D and accelerate their failure. Thus, imposing temporal regulation of insulin secretion mirroring the rest-activity cycles by alternated administration of ROR activator to ensure the insulin requirement during the day and ROR inhibitor during the resting state might represent a therapeutic strategy for improving insulin secretion in human T2D.

Materials and Methods

Human Islet Preparations. Human pancreatic islets were obtained from four different sources: 1) Prodo Laboratories LTD company (ND and T2D islets), 2) Alberta Diabetes Institute islet core center (ND and T2D islets), 3) Islet Transplantation Center of Geneva University Hospital (ND islets), and 4) Pancreatic Tissue Bank of Hospital Universitari de Bellvitge (ND islets). T2D donors had a history of T2D and HbA1c greater than 6.5%. Details of the islet donors are summarized in *SI Appendix*, Table S1. All procedures using human islets were approved by the ethical committee of Geneva University Hospital CCER 2017-00147.

Pancreatic Islet and Islet Cell Culture. Human pancreatic islets were cultured in Connaught Medical Research Laboratories (CMRL) 1066 medium, containing 5.5 mM or 20 mM glucose (where indicated) and supplemented with 10% FBS (Gibco), 110 U/mL penicillin (Gibco), 110 μg/mL streptomycin (Gibco), 50 μg/mL gentamicin (Gibco), 2 mM L-glutamine (GlutaMax, Gibco), and 1 mM sodium pyruvate (Gibco). Islet cell gentle dissociation was done using 0.05% Trypsin (Gibco) treatment. For bioluminescence recordings, 100 islets were plated to multiwell plates (LifeSystemDesign). For video time-lapse microscopy experiments, ∼20 human islets were plated to a 3.5-cm glass-bottom willco dish (WillCo Wells). For perifusion experiments on purified β-cells (Fig. 3*A*), ∼25,000 FACS-sorted β-cells were attached to 35-mm dishes (Falcon). For the rest of the experiments, ∼50,000 dissociated islet cells were attached to 35-mm dishes (Falcon). All dishes were precoated with a homemade laminin-5–rich extracellular matrix derived from 804G cells, as described in ref. 54.

Insulin Secretion Tests. Insulin secretion assays were performed on ∼50,000 attached islet cells. For GSIS assays, cells were washed in KRB solution (Krebs–Ringer bicarbonate) pH 7.4 supplemented with 0.3% free fatty acid BSA (Sigma) containing 2.8 mM glucose during 2 h, subsequently incubated for 1 h at 37 °C (basal condition), followed by 1-h stimulation with 16.7 mM glucose (stimulated condition), and additional 1-h incubation in KRB solution containing 2.8 mM glucose (rebasal condition). Next, 2.5 μM SR9011 (Sigma-Aldrich), or 20 μM Nobiletin (Sigma-Aldrich) were added where indicated. In the end of the experiments, cells were lysed in acid-ethanol solution (1.5% HCl and 75% ethanol) for 1 h at room temperature. For insulin release assay, cells were washed in serum-free CMRL medium supplemented with 0.5% fatty acidfree BSA (Sigma-Aldrich), and incubated in the same medium containing either 5.5 mM glucose or with 20 mM glucose (glucose-stimulated condition) for 7 h at 37 °C. Insulin was quantified in supernatants and cell lysates using a human insulin ELISA kit (Mercodia).

Viral Transduction and siRNA Transfection. Human islet cells were transduced with *Bmal1-luc*, *Per2-luc*, and RIP-GFP lentivectors, as described in ref. 12 and in *SI Appendix, Supplementary Methods*. Pppg-mCherry adenovirus was added at 10^5 fluorescence forming units (FFU)/islet (26) (see *SI Appendix, Supplementary Methods* for further details). Dissociated adherent human islet cells were transfected twice with 50 nM *siCLOCK* or with the same amount of nontargeting *siControl* (Dharmacon, GE Healthcare) (22, 23).

In Vitro Cell Synchronization and Circadian Bioluminescence Recording. Adherent islets were synchronized by a 1-h pulse of forskolin (10 μM; Sigma), 5 μM adrenaline (Geneva Hospital Pharmacy), 98 nmol/L Octreotide (Labatec Pharma), or 1.6 μM Liraglutide (Victoza), with a subsequent medium change. The islets were subjected to continuous bioluminescence recording in CMRL medium containing 100 μM luciferin (D-luciferin 306-250, NanoLight Technology) during several days (the experiment duration in hours is indicated in each graph). For the experiments with REV-ERB and ROR agonists, 2.5 μM SR9011 (Sigma-Aldrich) or 20 μM Nobiletin (Sigma-Aldrich), respectively, were applied together with forskolin synchronization pulse, and added to the recording medium for the entire experiment duration. For the experiments with high glucose, the CMRL medium was supplemented with 20 mM D-glucose (Sigma-Aldrich) from the synchronization step and during the entire recording. Bioluminescence pattern was monitored by a home-made robotic device equipped with photomultiplier tube detector assemblies, allowing the recording of 24-well plates (55). In order to analyze the amplitude of time series without the variability of magnitudes, raw data were processed in parallel graphs by moving average with a window of 24 h (22). Cell apoptosis was assessed where indicated with Cell Death Detection ELISA kit (Roche), according to manufacturer instructions.

Continuous Perifusion of Human Islet Cells. Human islet cells were transduced with the *Per2-luc* lentivectors, synchronized in vitro with a 1-h forskolin pulse, and placed into an in-house developed two-well horizontal perifusion chamber connected to the LumiCycle (23, 25). Cells were continuously perifused with sodium pyruvate-free CMRL supplemented with 10% FBS, 2 mM L-glutamine, 50 μg/mL gentamycin, 110 U/mL penicillin, 110 μg/mL streptomycin, 100 μM luciferin, and 5.5 mM glucose or 20 mM glucose. Bioluminescence recordings were performed in parallel to the 4-h interval automated collection of the outflow medium over 48 h. In the end of the

experiments, cells were lysed in acid-ethanol solution (1.5% HCl and 75% ethanol) for 1 h at room temperature. Insulin, glucagon, and proinsulin levels were quantified in the outflow medium using Human Insulin, Glucagon or Human Proinsulin Mercodia ELISA kits (Mercodia). The values were then normalized either to the residual intracellular content at the end of the experiment (48 h) (Figs. 3, 4, and 6*C*) or to the total RNA extracted from the nonperifused cells plated in parallel dishes (*SI Appendix*, Fig. S2 *D–F*).

Bioluminescence-Fluorescence Video Time-Lapse Microscopy. Human islets attached to glass-bottomed dishes (Willco Wells BV) were transduced with Pppg-mCherry adenovirus to label α-cells, RIP-GFP lentiviruses to label β-cells and with *Per2-luc* bioluminescence reporter. Islets synchronized by forskolin pulse were subjected to combined bioluminescence-fluorescence time-lapse microscopy (12) using Olympus LV200 workstation equipped with a 63× UPLSAPO objective and EM CCD camera (Image EM C9100-13, Hamamatsu). The recorded time-lapse images were analyzed on Fiji application (ImageJ), with individual cells tracked in the bioluminescence and fluorescence channels using a modified version of ImageJ plug-in CGE (27). Bioluminescence signal was measured over α- and β-cells within the encircled cell area (Fig. 2 *A* and *B* and Movies S1 and S2). Measuring of expression levels was performed on the labeled and tracked cells in the bioluminescence images over time. To assess the circadian characteristics of single-cell profiles, a JTK_Cycle fitting method was utilized (56).

TIRF Microscopy. Cells were imaged using a custom-built lens-type TIRF microscope based on an AxioObserver Z1 with a 100×/1.45 objective (Carl Zeiss). Excitation was from two DPSS lasers at 491 and 561 nm (Cobolt) passed through a clean-up filter (zet405/488/561/640x, Chroma) and controlled with an acousto-optical tunable filter (AA-Opto, France). Excitation and emission light were separated using a beamsplitter (ZT405/488/561/640rpc, Chroma). The emission light was chromatically separated onto separate areas of an EMCCD camera (Roper QuantEM 512SC) using an image splitter (Optical Insights) with a cutoff at 565 nm (565dcxr, Chroma) and emission filters (ET525/50m and 600/50m, Chroma). Scaling was 160 nm per pixel. Adenovirus-infected cells were imaged for 50 s at 100-ms exposure with 561 (0.2 to 0.5 mW) for exocytosis experiments in β-cells. Similarly, for α-cells the exposure was 561 (0.5 mW) and 491 (0.5 mW). Single images of cells were acquired to measure the number of docked granules at 100-ms exposure and 561 (0.2 mW) for β-cells and 561 (0.5 mW) and 491 (0.5 mW) for α-cells. Further details on the TIRF data analyses are presented in *SI Appendix, Supplementary Methods*.

Statistics. The results are expressed as means ± SEM for the indicated number of donors detailed in the figure legends, or illustrated as mean value of all experiments (average bioluminescence profiles). Statistical difference was tested by Student's *t* test to compare two groups. Paired Student's *t* test was applied when comparing different treatment for the same donor preparations, and nonpaired Student's *t* test to compare the values obtained with the islets from ND and T2D donors. Two-way ANOVA test with Bonferroni posttest was used to compare two dependent groups of continuous measurements, where indicated. All statistical tests were realized with GraphPad Prism 5 Software. Statistical significance was defined at $*P < 0.05$, $**P < 0.01$, and $***P < 0.001$. Correlation was quantified by Pearson coefficient *r*. To assess the circadian characteristics of hormone secretion or single-cell bioluminescence profiles, a JTK_Cycle fitting method was utilized (56). The profile was considered as circadian if adjusted *P* value was inferior to 0.1. The parameters of rhythmicity for bioluminescence recording experiments were evaluated based on the detrended values utilizing CosinorJ application.

ACKNOWLEDGMENTS. The authors thank Jacques Philippe, Ueli Schibler, and Claes Wollheim (University of Geneva) for constructive discussions; Marie-Claude Brulhart-Meynet (University Hospital of Geneva) for skillful technical assistance; Domenico Bosco and Thierry Berney (Islet Transplantation Center of Geneva University Hospital), Eduard Montanya Mias and Montserrat Nacher Garcia (Hospital Universitari de Bellvitge, Barcelona) for providing human islets; Etienne Lefai (Institut National de la Recherche Agronomique Auvergne Rhône-Alpes) for adenovirus amplification; Andre Liani and George Severi (University of Geneva) for assistance with perifusion experiments; and Christoph Bauer and Jerome Bosset (University of Geneva) for support with bioimaging experiments. Human islets from the Islet Transplantation Center of Geneva University Hospital were provided through Juvenile Diabetes Research Foundation Award 31-2008-416 (European Consortium for islet transplantation (ECIT) islet for Basic Research program, Thierry Berney). This work was funded by Swiss National Science Foundation Grants 31003A_166700/1, 310030_184708/1, the Vontobel Foundation, the Novartis Consumer Health Foundation, Bo and Kerstin Hjelt Foundation for diabetes type 2, Swiss Life Foundation, and the Olga Mayenfisch Foundation (C.D.); Swedish Research Council 2017-00956, 2018-02871 (to S.B. and A.T.); and Family Ernfors Foundation, European Foundation for the Study of Diabetes, Novo Nordisk Foundation, Diabetes Wellness Network Sweden, Swedish Diabetes Foundation, Exodiab network, Hjärnfonden (S.B.). N.R.G. was supported by the European Foundation for the Study of Diabetes–Rising Star Program and Novo Nordisk Foundation–Young Investigator Program.

1. C. Dibner, The importance of being rhythmic: Living in harmony with your body clocks. *Acta Physiol. (Oxf.)* **228**, e13281 (2020).
2. G. Asher, P. Sassone-Corsi, Time for food: The intimate interplay between nutrition, metabolism, and the circadian clock. *Cell* **161**, 84–92 (2015).
3. A. Kalsbeek, E. Fliers, Daily regulation of hormone profiles. *Handb. Exp. Pharmacol.* **217**, 185–226 (2013).
4. S. A. Brown, L. Gaspar, "Circadian metabolomics: Insights for biology and medicine" in *A Time for Metabolism and Hormones*, P. Sassone-Corsi, Y. Christen, Eds. (Cham, 2016), pp. 79–85.
5. F. Gachon, U. Loizides-Mangold, V. Petrenko, C. Dibner, Glucose homeostasis: Regulation by peripheral circadian clocks in rodents and humans. *Endocrinology* **158**, 1074–1084 (2017).
6. C. Dibner, U. Schibler, METABOLISM. A pancreatic clock times insulin release. *Science* **350**, 628–629 (2015).
7. M. Perelis *et al*., Pancreatic β cell enhancers regulate rhythmic transcription of genes controlling insulin secretion. *Science* **350**, aac4250 (2015).
8. B. Marcheva *et al*., Disruption of the clock components CLOCK and BMAL1 leads to hypoinsulinaemia and diabetes. *Nature* **466**, 627–631 (2010).
9. F. W. Turek *et al*., Obesity and metabolic syndrome in circadian Clock mutant mice. *Science* **308**, 1043–1045 (2005).
10. J. E. Gale *et al*., Disruption of circadian rhythms accelerates development of diabetes through pancreatic beta-cell loss and dysfunction. *J. Biol. Rhythms* **26**, 423–433 (2011).
11. L. Perrin *et al*., Transcriptomic analyses reveal rhythmic and CLOCK-driven pathways in human skeletal muscle. *eLife* **7**, e34114 (2018).
12. P. Pulimeno *et al*., Autonomous and self-sustained circadian oscillators displayed in human islet cells. *Diabetologia* **56**, 497–507 (2013).
13. R. Dallmann, A. U. Viola, L. Tarokh, C. Cajochen, S. A. Brown, The human circadian metabolome. *Proc. Natl. Acad. Sci. U.S.A.* **109**, 2625–2629 (2012).
14. E. C. Chua *et al*., Extensive diversity in circadian regulation of plasma lipids and evidence for different circadian metabolic phenotypes in humans. *Proc. Natl. Acad. Sci. U.S.A.* **110**, 14468–14473 (2013).
15. U. Loizides-Mangold *et al*., Lipidomics reveals diurnal lipid oscillations in human skeletal muscle persisting in cellular myotubes cultured in vitro. *Proc. Natl. Acad. Sci. U.S.A.* **114**, E8565–E8574 (2017).
16. J. T. Bass, The circadian clock system's influence in health and disease. *Genome Med.* **9**, 94 (2017).
17. C. Saini, S. A. Brown, C. Dibner, Human peripheral clocks: Applications for studying circadian phenotypes in physiology and pathophysiology. *Front. Neurol.* **6**, 95 (2015).
18. L. A. Sadacca, K. A. Lamia, A. S. deLemos, B. Blum, C. J. Weitz, An intrinsic circadian clock of the pancreas is required for normal insulin release and glucose homeostasis in mice. *Diabetologia* **54**, 120–124 (2011).
19. B. Marcheva, K. M. Ramsey, J. Bass, Circadian genes and insulin exocytosis. *Cell. Logist.* **1**, 32–36 (2011).
20. V. Petrenko *et al*., Pancreatic α- and β-cellular clocks have distinct molecular properties and impact on islet hormone secretion and gene expression. *Genes Dev.* **31**, 383–398 (2017).
21. V. Petrenko, C. Dibner, Cell-specific resetting of mouse islet cellular clocks by glucagon, glucagon-like peptide 1 and somatostatin. *Acta Physiol. (Oxf.)* **222**, e13021 (2018).
22. C. Saini *et al*., A functional circadian clock is required for proper insulin secretion by human pancreatic islet cells. *Diabetes Obes. Metab.* **18**, 355–365 (2016).
23. V. Petrenko, C. Saini, L. Perrin, C. Dibner, Parallel measurement of circadian clock gene expression and hormone secretion in human primary cell cultures. *J. Vis. Exp.*, e54673 (2016).
24. F. Sinturel *et al*., Cellular circadian period length inversely correlates with HbA_{1c} levels in individuals with type 2 diabetes. *Diabetologia* **62**, 1453–1462 (2019).
25. L. Perrin *et al*., Human skeletal myotubes display a cell-autonomous circadian clock implicated in basal myokine secretion. *Mol. Metab.* **4**, 834–845 (2015).
26. H. Shuai, Y. Xu, Q. Yu, E. Gylfe, A. Tengholm, Fluorescent protein vectors for pancreatic islet cell identification in live-cell imaging. *Pflugers Arch.* **468**, 1765–1777 (2016).
27. D. Sage, M. Unser, P. Salmon, C. Dibner, A software solution for recording circadian oscillator features in time-lapse live cell microscopy. *Cell Div.* **5**, 17 (2010).
28. N. R. Gandasi *et al*., Glucose-dependent granule docking limits insulin secretion and is decreased in human type 2 diabetes. *Cell Metab.* **27**, 470–478.e4 (2018).
29. S. Barg, M. K. Knowles, X. Chen, M. Midorikawa, W. Almers, Syntaxin clusters assemble reversibly at sites of secretory granules in live cells. *Proc. Natl. Acad. Sci. U.S.A.* **107**, 20804–20809 (2010).
30. N. R. Gandasi *et al*., Survey of red fluorescence proteins as markers for secretory granule exocytosis. *PLoS One* **10**, e0127801 (2015).
31. S. Del Guerra *et al*., Functional and molecular defects of pancreatic islets in human type 2 diabetes. *Diabetes* **54**, 727–735 (2005).

32. B. He *et al*., The small molecule nobiletin targets the molecular oscillator to enhance circadian rhythms and protect against metabolic syndrome. *Cell Metab.* **23**, 610–621 (2016).
33. L. A. Solt *et al*., Regulation of circadian behaviour and metabolism by synthetic REV-ERB agonists. *Nature* **485**, 62–68 (2012).
34. V. Petrenko, J. Philippe, C. Dibner, Time zones of pancreatic islet metabolism. *Diabetes Obes. Metab.* **20** (suppl. 2), 116–126 (2018).
35. T. Hirota *et al*., Glucose down-regulates Per1 and Per2 mRNA levels and induces circadian gene expression in cultured Rat-1 fibroblasts. *J. Biol. Chem.* **277**, 44244–44251 (2002).
36. S. J. Aton, E. D. Herzog, Come together, right...now: Synchronization of rhythms in a mammalian circadian clock. *Neuron* **48**, 531–534 (2005).
37. M. A. Ravier *et al*., Loss of connexin36 channels alters beta-cell coupling, islet synchronization of glucose-induced Ca2+ and insulin oscillations, and basal insulin release. *Diabetes* **54**, 1798–1807 (2005).
38. R. Rodriguez-Diaz *et al*., Paracrine interactions within the pancreatic islet determine the glycemic set point. *Cell Metab.* **27**, 549–558.e4 (2018).
39. J. A. Stamenkovic *et al*., Regulation of core clock genes in human islets. *Metabolism* **61**, 978–985 (2012).
40. A. C. Liu *et al*., Intercellular coupling confers robustness against mutations in the SCN circadian clock network. *Cell* **129**, 605–616 (2007).
41. Z. Chen *et al*., Identification of diverse modulators of central and peripheral circadian clocks by high-throughput chemical screening. *Proc. Natl. Acad. Sci. U.S.A.* **109**, 101–106 (2012).
42. N. Lawlor *et al*., Single-cell transcriptomes identify human islet cell signatures and reveal cell-type-specific expression changes in type 2 diabetes. *Genome Res.* **27**, 208–222 (2017).
43. A. H. Rosengren *et al*., Overexpression of alpha2A-adrenergic receptors contributes to type 2 diabetes. *Science* **327**, 217–220 (2010).
44. B. Thorens, GLUT2, glucose sensing and glucose homeostasis. *Diabetologia* **58**, 221–232 (2015).
45. G. Boden, J. Ruiz, J. L. Urbain, X. Chen, Evidence for a circadian rhythm of insulin secretion. *Am. J. Physiol.* **271**, E246–E252 (1996).
46. A. Fritsche *et al*., Relationships among age, proinsulin conversion, and beta-cell function in nondiabetic humans. *Diabetes* **51** (suppl. 1), S234–S239 (2002).
47. M. Ruiter *et al*., The daily rhythm in plasma glucagon concentrations in the rat is modulated by the biological clock and by feeding behavior. *Diabetes* **52**, 1709–1715 (2003).
48. G. Boden, X. Chen, M. Polansky, Disruption of circadian insulin secretion is associated with reduced glucose uptake in first-degree relatives of patients with type 2 diabetes. *Diabetes* **48**, 2182–2188 (1999).
49. S. A. Andersson *et al*., Reduced insulin secretion correlates with decreased expression of exocytotic genes in pancreatic islets from patients with type 2 diabetes. *Mol. Cell. Endocrinol.* **364**, 36–45 (2012).
50. D. J. Stenvers, F. A. J. L. Scheer, P. Schrauwen, S. E. la Fleur, A. Kalsbeek, Circadian clocks and insulin resistance. *Nat. Rev. Endocrinol.* **15**, 75–89 (2019).
51. Y. S. Lee *et al*., Nobiletin improves obesity and insulin resistance in high-fat diet-induced obese mice. *J. Nutr. Biochem.* **24**, 156–162 (2013).
52. E. E. Mulvihill *et al*., Nobiletin attenuates VLDL overproduction, dyslipidemia, and atherosclerosis in mice with diet-induced insulin resistance. *Diabetes* **60**, 1446–1457 (2011).
53. K. Nohara *et al*., Nobiletin fortifies mitochondrial respiration in skeletal muscle to promote healthy aging against metabolic challenge. *Nat. Commun.* **10**, 3923 (2019).
54. G. Parnaud *et al*., Proliferation of sorted human and rat beta cells. *Diabetologia* **51**, 91–100 (2008).
55. A. Gerber *et al*., Blood-borne circadian signal stimulates daily oscillations in actin dynamics and SRF activity. *Cell* **152**, 492–503 (2013).
56. M. E. Hughes, J. B. Hogenesch, K. Kornacker, JTK_CYCLE: An efficient nonparametric algorithm for detecting rhythmic components in genome-scale data sets. *J. Biol. Rhythms* **25**, 372–380 (2010).